IEEE Access
Multidisciplinary | Rapid Review | Open Access Journal

Received 23 July 2024, accepted 4 August 2024, date of publication 13 August 2024, date of current version 22 August 2024.

Digital Object Identifier 10.1109/ACCESS.2024.3443210

RESEARCH ARTICLE

Design and Characterization of Twisted and Coiled Polymers and Their Applications as Soft Actuators

JACOB MARTIN AND MARC DOUMIT
Department of Mechanical Engineering, University of Ottawa, Ottawa, ON K1N 6N5, Canada
Corresponding author: Jacob Martin (jmart231@uottawa.ca)

ABSTRACT This study is an experimental investigation of twisted and coiled polymer actuators, focusing on characterization of the effects of design and operating parameters on the actuator performance. Using nylon-6 monofilaments, a custom fabrication and testing setup was designed to enable control of the operating conditions, precursor fiber diameter, actuator spring index, motor speed, training conditions, coil bias angle, pre-stretch of the precursor fiber, and pre-stretch of the actuator. Isotonic, isometric, and eccentric contraction tests were performed to evaluate each parameter's effects on actuator stroke, force, and range in variable stiffness. Results demonstrate that optimal actuator performance is influenced by the operating conditions, selection of precursor fiber diameter, spring index, coil bias angle, training conditions, and the magnitude of pre-stretch in the precursor fiber and fully coiled actuator. This comprehensive experimental evaluation aims to assist in the optimization of twisted and coiled polymer actuators tailored to specific stroke, force, and variable stiffness performance requirements.

INDEX TERMS Actuators, artificial muscles, smart materials, soft robotics, twisted coiled polymer actuators, variable stiffness.

I. INTRODUCTION

Research into soft actuation technologies has gained significant attention due to the applications in fields like soft robotics and human mobility assistive devices [1]. Smart materials, such as twisted and coiled polymer (TCP) actuators, offer promising solutions with advantages over conventional actuators including their inherent ability to deform or reconfigure in response to external stimuli, scalability, simplicity, and low cost [2]. Haines et al. [3] first demonstrated this concept by twisting and subsequently coiling a nylon 6,6 monofilament after a critical number of twists were inserted into the fiber. When varying the spring index, C, defined as the ratio of the coil diameter to the precursor fiber diameter, the authors demonstrated a TCP stroke of 49% at 1 MPa for $C = 5.5$. Conversely at $C = 1.1$, the authors demonstrated repeatable TCP strokes at 50 MPa, but with a reduced maximum stroke of 9.3%.

The associate editor coordinating the review of this manuscript and approving it for publication was Tao Wang.

Recent research has primarily focused on modelling and control [4], [5], [6], upscaling performance through bundling [7], [8], [9], or real-world applications of TCP actuators including robotics and assistive devices [10], [11]. Studies have investigated TCP performance, including force generation, tensile stroke, and range in stiffness, identifying key design considerations. Aziz et al. [12] explored the effects of precursor fiber diameter, twist density, and coil bias angle on non-coiled fibers, and demonstrated increased stroke and torque with higher twist levels. However, this study did not evaluate tensile performance in fully coiled actuators. In another study, Aziz et al. [13] attributed torsional performance to the differences in anisotropic thermal expansion between the fibers. While the effects of improving anisotropy in thermal expansion have not been extensively studied, it has been suggested that drawing or pre-stretching precursor fibers, or using materials with greater anisotropic properties, can enhance TCP performance [5], [14], [15].

Saharan and Tadesse [16] studied the effects of twist insertion speed on actuator performance. While changes in

performance were observed for samples fabricated between 200 rpm and 1800 rpm, the changes did not scale as expected and the authors recommended further research is required. Other studies [1], [17], [18] indicated that training conditions such as the static load used, or use of mechanical springs, can affect the actuator performance during testing. To date, however, relationships between the training conditions and actuator performance have not been adequately characterized.

Li et al. [19] characterized the effects of controlling the annealing stress on the actuator stroke. The authors demonstrated contraction strain can be improved by increasing the annealing stress, but the results were limited to isotonic testing and did not evaluate the effects on force generation or range in stiffness. Additionally, detailed fabrication and testing parameters were missing that are required to enable proper performance comparison.

Several authors [3], [20], [21] identified a steep segment of the load-deformation curve at elevated temperatures, sometimes termed the preload knee, where TCP samples exhibit higher stiffness due to neighboring coil contact. Cherubini et al. [20] reported a change in modulus from 78-101 MPa between 25° and 122°; however, factors that may contribute to the steepness of the preload knee region were not investigated in this study. Similarly, Li et al. [21] investigated the effects of varying the pre-stretch during testing on the range of achievable stiffness. The authors reported an optimal range of pre-stretch loading conditions that yield the greatest range and ratio in stiffness; however, they acknowledged that future work was required to characterize what other factors may influence the range in stiffness. Additional improvements are also needed in areas related to selection of precursor fibers, assessing the influence of some manufacturing parameters (fabrication load, heat treatment conditions), dynamic behavior, and methods for tuning the temperature at which neighboring TCP coils are in contact.

In summary, although research on TCP actuators encompasses modeling, control, and applications, critical design, fabrication, and operational parameters that influence performance metrics such as stroke, force generation, and stiffness remain inadequately characterized. Inconsistent reporting metrics and experimental methodologies highlight the need for more robust and uniform approaches to ensure comprehensive and reliable results. This work aims to systematically investigate these design and operating parameters, offering a foundation for optimizing TCPs tailored to specific applications with precise requirements. Moreover, the literature inadequately explores the factors affecting variable stiffness properties of TCP actuators, making it a focus area for the present work.

II. MATERIALS AND METHODS

This study aims to provide a comprehensive and consistent experimental evaluation of TCP actuators, focusing on eight fabrication and operating parameters and their effects on the tensile stroke, force generation, and range in stiffness. Using nylon-6 monofilament and a custom fabrication apparatus (Fig. 1), TCP actuators were fabricated with consistent parameters and tested under isotonic, isometric, and eccentric contractions. The monofilaments selected were Trilene Big Game fishing lines from Berkley Fishing [22] in break strengths of 10 lb, 15 lb, 25 lb, and 50 lb, corresponding to average fiber diameters of 0.21 mm, 0.38 mm, 0.48 mm, and 0.71 mm, respectively.

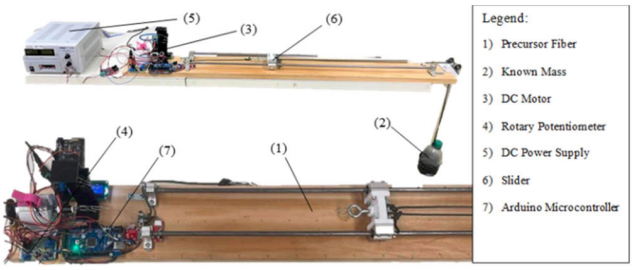

FIGURE 1. Automated fabrication setup for twisting and coiling (top); Close up view of precursor fiber prior to twist insertion (bottom).

In addition to the custom fabrication apparatus, three experimental setups were designed to enable control of various design parameters including the operating conditions, precursor fiber diameter, spring index, twist density and coil bias angle, twist insertion speed, training load, amount of pre-stretch in the precursor fiber prior to twisting, and the amount of pre-stretch in the coiled samples during annealing. The fabrication apparatus was validated by creating TCP prototypes with consistent properties and testing their performance to ensure consistency between samples.

The fabrication process of TCP actuator prototypes followed a four-step procedure. A precursor fiber (1) is fixed at both ends of the fabrication apparatus and is loaded with a chosen mass (2) on the opposite side of the slider (6). A DC motor (3) inserts twists in the fiber at a speed controlled by a rotary potentiometer (4) and continues until the fiber has fully twisted and coiled along its length. The number of twists inserted into the fiber is displayed on the LCD screen. The prototype is then placed on a wire rack in an Instron environmental chamber to anneal at 160° for two hours to set the coiled structure and relieve any residual stresses. Finally, the prototypes are trained in the Instron environmental chamber under expected actuator operating loads until consistent cycles have been achieved.

Three experimental setups were designed to evaluate isotonic, isometric, and eccentric contractions using an Instron 4202 universal tensile testing machine with a 500 N load cell and precision of $\pm$ 0.1 N [23], along with a Watlow T-series thermocouple with an accuracy of $\pm$ 1° [24]. During isotonic testing (Fig. 2), TCP actuators were coupled to a linear variable differential transformer (LVDT) with a 0-150 mm working range, infinite resolution, and $\pm$ 0.5% linearity [25]. Masses were suspended from the coupled ends and TCP contraction was recorded by the LVDT as the samples were heated. During isometric contraction (Fig. 3), both ends of

the TCP prototypes were fixed, and the generated force was recorded by the Instron load cell as the actuators were heated. Eccentric contraction testing used a similar setup (Fig. 3), except the temperature of the actuator was controlled instead of its length. Actuators were heated to constant temperatures while the Instron machine performed load-unload tests to capture force and displacement data. All experimental data was recorded in LabVIEW and processed in MATLAB.

FIGURE 2. Experimental setup for isotonic contractions. Instron environmental chamber with linear variable differential transformer inserted at the top of the chamber (left); Inside view of environmental chamber during actuation (right).

FIGURE 3. Experimental setup for isometric and eccentric contractions. Instron environmental chamber with support fixed to TCP sample at the lower end, and to the Instron load cell at the top end (left); b) Inside view of environmental chamber during actuation with TCP sample ends fixed (right).

III. RESULTS

A. ISOTONIC CONTRACTION TESTING

During isotonic testing, prototypes were prepared following the protocols discussed in Section II. All fabrication and operating parameters were consistent apart from the varied parameter under investigation. Samples were heated from 45° to 200°, while temperature and displacement data were recorded. Unless otherwise indicated, the static masses suspended from the prototypes were adjusted to achieve an actuating stress of approximately 17.50 MPa, where stress is calculated as the load normalized with the initial precursor fiber cross-sectional area. Tensile stroke is calculated as the change in TCP length divided by the initial length. A summary of the isotonic contraction testing is presented in Table 1, while graphs comparing the effects on TCP stroke are presented in Appendix A.

TABLE 1. Summary of isotonic contraction testing and the effects of design parameters on tensile stroke.

Design Parameter	Change	Effect on Tensile Stroke
Actuating Load	Increase in Applied Load	Optimal load of 3.60 N yields largest stroke
Precursor Fiber Diameter	Increase in Diameter	No change if actuating stress is constant
Spring Index	Increase in Spring Index	Increase from 8.2% to 13.5%
Coil Bias Angle	Increase in Coil Bias Angle	Increase from 10.0% to 14.0%
Twist Insertion Speed	Increase in Twist Insertion Speed	Negligible effect
Training Conditions	Increase in Mass (Static)	Minimal effect if actuating load kept constant
	Increase in Spring Constant (Dynamic)	Minimal effect after initial sets of testing
Pre-stretching Precursor Fiber	Increase in Precursor Fiber Pre-stretch	Increase from 9.7% to 16.4%
Pre-stretching Coiled Sample	Increase in Pre-stretch of Coiled Sample	Increase from 9.7% to 12.8%

The effects of the operating conditions on the tensile stroke capacity were evaluated by fabricating two samples with consistent properties and testing them under isotonic conditions against 1.38 N, 2.72 N, 3.60 N, 4.94 N, and 7.17 N loads. Results demonstrate an optimal load was required to achieve maximum tensile stroke, where the largest mean stroke of 15.91% (standard deviation, SD = 0.39%) was achieved for the 3.60 N load (Fig.4).

Next, four samples were fabricated using each of the precursor fiber diameters and were twisted and coiled under consistent applied stress. During isotonic testing, all samples achieved an average of 16.25% (SD = 0.36%) stroke when heated from 45° to 200° (Fig.5).

The effects of the spring index on the actuator tensile stroke were investigated by fabricating samples at C = 2.17, C = 2.02, and C = 1.94, and testing them under isotonic conditions. The samples with the largest spring index achieved the greatest tensile stroke at an average of 13.55% (SD = 0.19%). In contrast, the samples with the lowest spring index achieved an average of 8.31% (SD = 0.57%) (Fig.6).

Varying levels of twist density were also investigated, with coil bias angles measured using a microscope with 200 times magnification. Twist density was varied by manually inserting additional twists into the TCP after the samples had fully coiled. The measured coil bias angles for the samples with high, medium, and low twist densities were 21°, 25°, and 30°, respectively. For the samples with the lowest coil bias angle, tensile stroke reached an average of 10.10% (SD = 0.15%). In comparison, the samples with the highest coil bias angle achieved an average tensile stroke of 13.94% (SD = 0.25%) (Fig.7).

The effects of the twist insertion speed on the actuator stroke were investigated by fabricating samples with consistent properties at four motor speeds of approximately 60 rpm, 240 rpm, 480 rpm, and 720 rpm. The prototypes were tested

under isotonic conditions while heating from 45° to 200°. In all cases, tensile stroke reached an average of 12.95% (SD = 0.10%) when actuating against the same external load of 3.17 N (Fig.7).

The effects of the training conditions on the tensile stroke were evaluated by fabricating five sets of samples with consistent properties and training under different static and dynamic conditions. Three sets of samples were trained against static loads of 1.83 N, 3.60 N, and 4.94 N, while the remaining sets were tested under dynamic conditions against extension springs with constants (k) of 0.0319 N/mm and 0.0929 N/mm. When actuating against the same external load of 3.17 N, all samples achieved an average tensile stroke of 14.98% (SD = 0.50%) after the third test trial, irrespective of the training load or condition used (Fig.8).

The effects of pre-stretching the precursor fiber and increasing the anisotropy in thermal expansion were investigated by stretching precursor fibers to 2.5%, 5%, and 7.5% strain such that the final measured lengths were approximately 210 mm. The precursor fibers were annealed at 80° for 4 hours and left to cool for 24 hours prior to twisting and coiling. When actuating against the same external load of 3.17 N, samples with the lowest amount of pre-stretch achieved an average of 9.82% (SD = 0.21%) stroke, while samples with the highest amount of pre-stretch generated an average of 16.28% (SD = 0.29%) stroke (Fig.10).

Lastly, the effects of pre-stretching the fully coiled TCP samples while annealing on the actuator stroke were investigated. Samples were fabricated with consistent properties, stretched to approximately 7.5%, 21%, and 35% strain, and fixed to a wire rack during annealing. The samples retained their coiled structure after 3 hours of annealing at 170°. When testing the prototypes under isotonic conditions, the samples with the lowest amount of pre-stretch achieved an average of 9.75% (SD = 0.28%) stroke, while the samples with the highest amount of pre-stretch reached an average of 12.83% (SD = 0.03%) stroke when actuating against the same external load (Fig.11).

B. ISOMETRIC CONTRACTION TESTING

To capture the effects of altering different fabrication and operating parameters on the actuator force generation, a series of experiments were conducted following the isometric experimental setup. Samples were fixed to the aluminum rods while removing any slack or tension, and subsequently heated from 45° to 200°. A summary of the isometric contraction testing is presented in Table 2, while graphs comparing the effects on TCP force are presented in Appendix B.

The effects of the operating conditions were evaluated by measuring the generated force for samples with no initial extension or preload, as well as preloads with magnitudes of 0.5 N, 0.75 N, 1.0 N, 1.25 N, and 1.5 N. Isometric testing results demonstrate the samples with the largest preload achieved an average generated force of 1.36 N (SD = 0.10 N), while introducing no preload (blocked force) resulted in the largest generated force of 2.50 N (SD = 0.12 N) (Fig.12).

TABLE 2. Summary of isometric contraction testing and the effects of design parameters on TCP force generation.

Design Parameter	Change	Effect on Force Generation
Actuating Load	Increase in Applied Load	Decrease from 2.50 N to 1.36 N
Precursor Fiber Diameter	Increase in Diameter	Increase from 0.81 N to 6.60 N
Spring Index	Increase in Spring Index	Decrease from 2.95 N to 1.79 N
Coil Bias Angle	Increase in Coil Bias Angle	Decrease from 2.10 N to 1.48 N
Twist Insertion Speed	Increase in Twist Insertion Speed	Negligible effect
Training Conditions	Increase in Mass (Static)	Increase from 1.70 N to 2.72 N
	Increase in Spring Constant (Dynamic)	Increase from 1.86 N to 2.57 N
Pre-stretching Precursor Fiber	Increase in Precursor Fiber Pre-stretch	Decrease from 1.98 N to 1.53 N
Pre-stretching Coiled Sample	Increase in Pre-stretch of Coiled Sample	Decrease from 1.88 N to 1.48 N

The blocked force was also measured for samples fabricated with different precursor fiber diameters. After the samples were heated from 45° to 200°, the samples with a precursor fiber diameter of 0.21 mm generated an average blocked force of 0.81 N (SD = 0.04 N). In contrast, the samples with a precursor fiber diameter of 0.71 mm achieved an average of 6.60 N (SD = 0.38 N) of blocked force (Fig.13).

Next, the effects of varying the spring index on the actuator force generation were investigated through isometric testing. Results demonstrate the samples with the highest spring index of 2.17 achieved the lowest average blocked force of 1.79 N (SD = 0.04 N), whereas the samples with the lowest spring index of 1.94 achieved an average of 2.95 N (SD = 0.06 N) (Fig.13).

The samples fabricated with varying coil bias angles were tested under isometric conditions to evaluate the effects on the generated force. The samples with the highest twist density and lowest coil bias angles (21°) achieved an average of 2.10 N (SD = 0.10 N) of blocked force. In contrast, the samples with the lowest twist density and largest coil bias angles (30°) recorded an average blocked force of 1.48 N (SD = 0.05 N) (Fig.14).

The effects of the twist insertion speed on the actuator generated force were investigated under isometric conditions. All samples achieved repeatable blocked forces averaging 1.74 N (SD = 0.04 N), regardless of the motor speeds of 60 rpm, 240 rpm, 480 rpm, and 720 rpm used during fabrication (Fig.15).

Next, the effects of the training conditions on the actuator force generation were investigated. For the samples trained against static masses, the smallest forces were produced by the samples trained against the 1.83 N load, achieving an average of 1.70 N (SD = 0.04 N) of blocked force. The generated forces were largest for the samples trained against the 4.94 N load, achieving an average of 2.72 N (SD = 0.02 N) of blocked force. Similarly, for the samples trained under

dynamic conditions (Fig.16), the samples trained against the lower spring constant generated an average of 1.86 N (SD = 0.00 N) of blocked force while the samples trained against the higher spring constant generated an average of 2.57 N (SD = 0.03 N).

The samples fabricated with varying levels of pre-stretch in the precursor fiber were tested under isometric conditions to investigate the effects of precursor fiber anisotropy on the actuator force generation. Here, the samples with the largest amount of pre-stretch (7.5%) generated the lowest blocked forces at an average of 1.53 N (SD = 0.01 N). In contrast, the samples with the lowest amount of pre-stretch (2.5%) generated the greatest blocked forces (Fig.17) at an average of 1.98 N (SD = 0.02 N).

Lastly, the prototypes fabricated with varying magnitudes of pre-stretch in the coiled samples during the annealing stage were tested under isometric conditions. The largest forces were observed for the samples with the smallest magnitude of pre-stretch (7.5%) at an average of 1.88 N (SD = 0.05 N), while the samples stretched to 35% achieved the lowest forces at an average of 1.48 N (SD = 0.01 N) (Fig.18).

C. ECCENTRIC CONTRACTION TESTING

To capture the effects of altering different fabrication and operating conditions on the actuator variable stiffness properties, a series of experiments were conducted following the eccentric experimental setup. Samples were fixed to the aluminum rods while removing any slack or tension, and subsequently brought to constant temperatures (including room temperature, 50°, 80°, and 110°) in the environmental chamber. The range in stiffness was calculated as the ratio of the maximum to minimum elastic moduli, and all stresses were calculated by normalizing the effective generated force with the initial precursor fiber cross-sectional area. A summary of the eccentric contraction testing is presented in Table 3, while graphs comparing the effects on TCP range in stiffness are presented in Appendix C.

TABLE 3. Summary of eccentric contraction testing and the effects of design parameters on TCP range in stiffness.

Design Parameter	Change	Effect on Range in Stiffness
Strain Rate	Increase in Strain Rate	Increase from 2.13 to 2.31
Spring Index	Increase in Spring Index	Increase from 1.63 to 1.69
Coil Bias Angle	Increase in Coil Bias Angle	Increase from 1.44 to 3.16
Pre-Stretching Precursor Fiber	Increase in Precursor Fiber Pre-stretch	Increase from 1.92 to 2.13
Pre-Stretching Coiled Sample	Increase in Pre-stretch of Coiled Sample	Decrease from 1.45 to 1.33

First, the effects of the operating conditions on the actuator range in stiffness were tested by loading the TCP samples to 5% strain at strain rates of 2-, 5-, and 10 mm/min, and measuring the tensile modulus at each temperature. Results demonstrate that the minimum average modulus was measured at room temperature, while the maximum modulus was measured at 110°, for all strain rates. The range in stiffness factor was greatest at 2.31 for the strain rates of 10 mm/min. In contrast, the range in stiffness factor was lowest at 2.13 for the slowest strain rates of 2 mm/min. To conserve time and ensure consistency in the data captured, a 5 mm/min strain rate was selected for all remaining eccentric tests (Fig.19).

The effects of the spring index on the variable stiffness properties of the actuators were tested for the samples with a spring index of 2.17, 2.02, and 1.94. The range in stiffness factor was highest at 1.69 for the samples with spring indices of 2.17. In contrast, the range in stiffness decreased to 1.63 for samples fabricated with spring indices of 1.94 (Fig.21).

For the samples fabricated with varying twist densities and coil bias angles, the average modulus at room temperature was 115.77 MPa (SD = 3.23 MPa) for the samples with 30° coil bias angles, and 270.96 MPa (SD = 2.05 MPa) for the samples with 21° bias angles (Fig.22). When heated to 110°, the range in stiffness factor was 3.16 for the samples with the largest coil bias angles, and 1.44 for the samples with the lowest coil bias angles.

Next, the samples fabricated with varying magnitudes of pre-stretch in the precursor fiber were investigated for its effects on the range in stiffness. Results demonstrate the range in stiffness factor was lowest at 1.92 for the samples with 2.5% pre-stretch in the precursor fiber. The range in stiffness factor increased to 2.12 at 5% pre-stretch, with a slight increase to 2.13 at 7.5% pre-stretch (Fig.26).

Lastly, the range in stiffness factor was evaluated for samples fabricated with varying levels of pre-stretch introduced to the coiled samples during the annealing stage. At the lowest pre-stretch of 7.5%, a range in stiffness factor of 1.45 was measured. In comparison, at the highest pre-stretch of 35%, the measured variation in stiffness factor was 1.33 (Fig.27).

IV. DISCUSSION

Analysis of the isotonic test results revealed several relationships between individual design parameters and their effects on actuator stroke. An optimal actuating load exists that yields the maximum tensile stroke, where insufficient loads result in inadequate space between neighboring coils to contract. In contrast, higher actuating loads create opposing forces that are too large for the actuator to overcome. Pre-stretching the precursor fiber, as well as the TCP during annealing, was effective at improving the TCP stroke. Conversely, actuator stroke was limited in samples prepared with higher coiling loads (and low spring indices), or if the twist density of the actuator was increased reducing the coil bias angle. Actuator stroke was independent of the precursor fiber diameter used if the stresses were consistent between samples, and the motor speed used during fabrication also had a negligible effect on the actuator stroke. Adjusting the actuator training load did not influence tensile stroke after the third test trial, although a minor re-training step was required when altering the actuating load to obtain consistent actuation cycles.

Isometric tests provided further insight into the effects of each parameter on the actuator force generation. The generated force increased notably with increasing precursor fiber diameter. While the precursor fiber diameter had a minimal effect on the actuator stroke, it had a noticeable effect on the actuator force generation and should be considered carefully in the design. Training techniques, using heavier static masses or stiffer extension springs, were effective at improving the actuator force. The twist insertion speed, similar to the isotonic test results, had a negligible effect on the actuator force generation. In contrast, lower coiling loads (and higher spring indices) reduced the effective force generation of the actuator, presenting a trade-off in performance with the actuator stroke. Similar trade-offs were observed when varying the twist density and coil bias angle, where samples with higher twist densities and lower coil bias angles achieved the largest blocked forces. Moreover, pre-stretching either the precursor fiber or the coiled actuator during the annealing stage limited the actuator force generation, highlighting additional trade-offs in performance between actuator stroke and generated force.

The final performance metric evaluated was the range in stiffness. In all cases, nominal moduli of the TCPs decreased with increasing temperature until neighboring coils contacted, after which the nominal moduli tended to increase by a factor dependent on the parameter under investigation. Higher strain rates yielded wider ranges in stiffness indicating a sensitivity to dynamic loading conditions. Pre-stretching the precursor fiber showed a general increasing trend in the magnitude of the range in stiffness; however, the minimal change between 5% and 7.5% pre-stretch indicates that further tests using broader pre-stretch ranges may be required to fully establish this relationship. Conversely, decreasing trends were observed in the range in stiffness as the spring index or coil bias angle decreased; however, it is worth noting that the stresses required to elongate the samples were considerably higher at all temperatures for samples with the lowest spring index and lowest coil bias angle, potentially contributing to the narrower ranges in stiffness. Similarly, a decreasing trend was observed in the range in stiffness when increasing the pre-stretch in the coiled samples, highlighting a reduction in the actuators' effective force capacity and strength during operation. Designers should avoid excessive twist density and pre-stretching of the TCP beyond what is required to meet the stroke requirements, in order to maintain a wider range in stiffness.

V. CONCLUSION AND FUTURE WORK

The objective of this work was to comprehensively characterize the mechanical and thermal performance of TCP actuators, facilitating the fabrication of tailored prototypes meeting specific design criteria or requirements. Eight fabrication and operating parameters were identified that lacked characterization collectively for their potential effects on the actuator performance, namely the stroke, force generation, and range in stiffness. Strategies to enhance stroke capacity include optimizing the actuating load, increasing the spring index, and pre-stretching the precursor fiber to improve the thermal anisotropy. To improve the force generation, designers can consider minimizing the preload, increasing the precursor fiber diameter, reducing the spring index, training against heavier masses or stiffer extension springs, and avoiding additional pre-stretch to the precursor fiber or fully coiled sample. To achieve wider ranges in stiffness, some methods include increasing the strain rate, limiting twist density and increasing coil bias angle, and increasing the spring index.

In future work, several key areas need to be addressed to enhance the understanding and applications of TCP actuators. While this study provides valuable insights for designers intending to optimize TCP actuator performance for high stroke, force, or variable stiffness applications, most practical applications would involve a combination of these performance metrics. A comprehensive analysis of the interaction effects between multiple parameters is critical for finding the optimal combination of design parameters that yield the desired set of performance requirements, while minimizing the negative effects of any trade-offs. The study should also be expanded to encompass a broader range of environmental conditions, such as varying humidity levels, to assess their influence on TCP performance. Before adopting TCP actuators into various applications, the long-term durability and cycle performance of TCPs under diverse operating conditions should be investigated to confirm that TCPs can maintain their performance requirements over time. Moreover, the scalability of TCP actuators should be explored for applications such as robotics and mobility assistive devices, ensuring the optimized parameters are consistently reproducible at a larger scale. Finally, the use of advanced materials, including alternative precursor polymers and composite materials, should be studied to identify potential candidates that may offer superior performance to those studied in this work. These future areas of work should collectively advance the field and contribute to the development of more robust and versatile TCP actuators.

APPENDIX A
COMPLETE ISOTONIC TESTING RESULTS

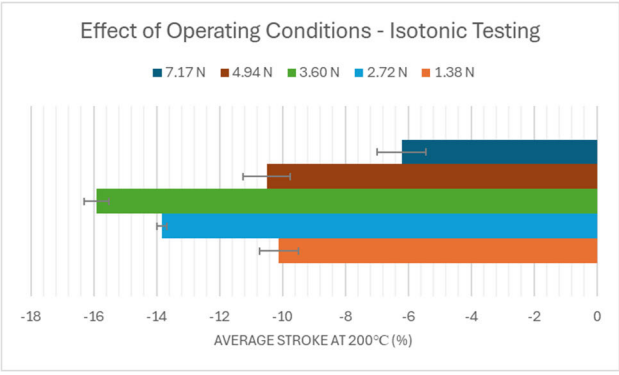

FIGURE 4. Effect of operating load on TCP stroke.

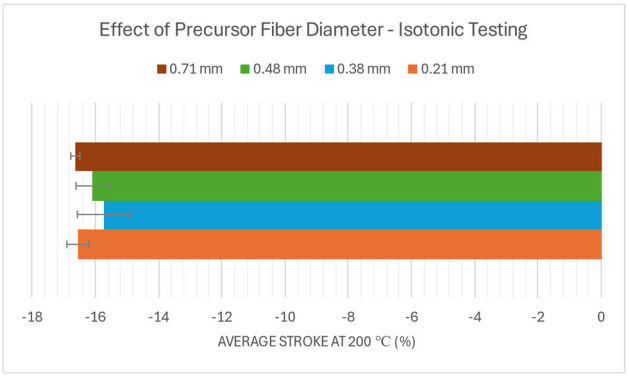

FIGURE 5. Effect of precursor fiber diameter on TCP stroke.

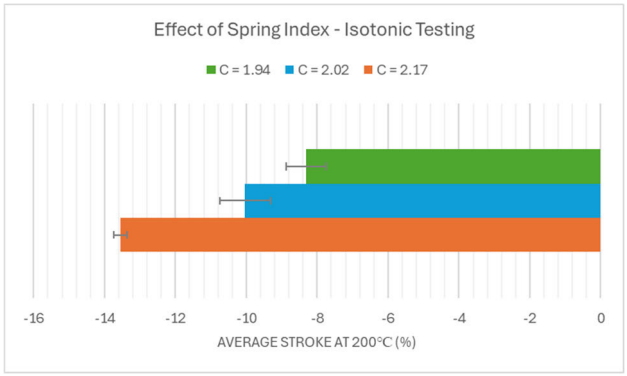

FIGURE 6. Effect of spring index on TCP stroke.

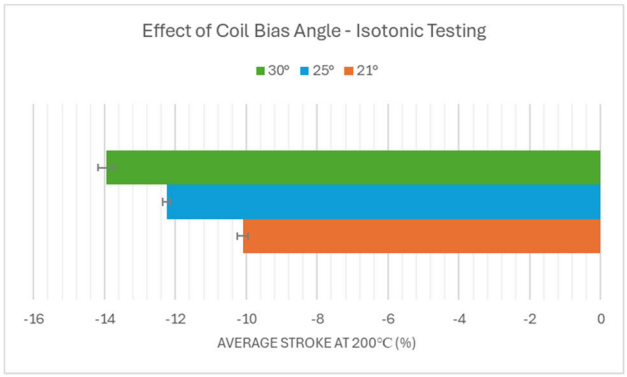

FIGURE 7. Effect of twist density and coil bias angle on TCP stroke.

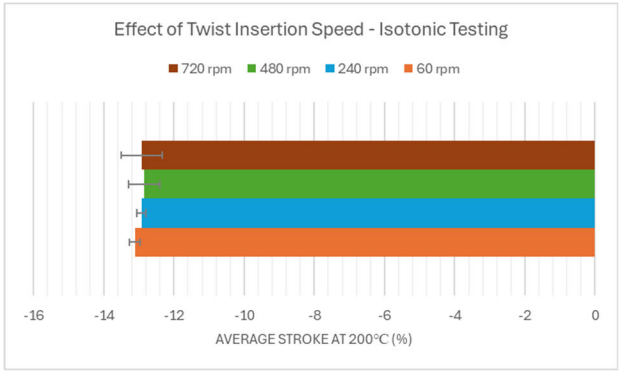

FIGURE 8. Effect of twist insertion speed on TCP stroke.

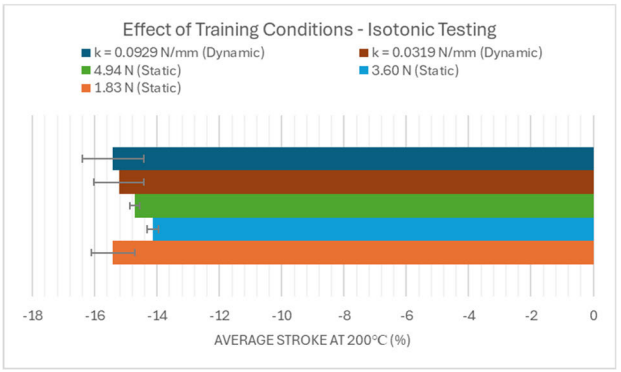

FIGURE 9. Effect of training conditions on TCP stroke.

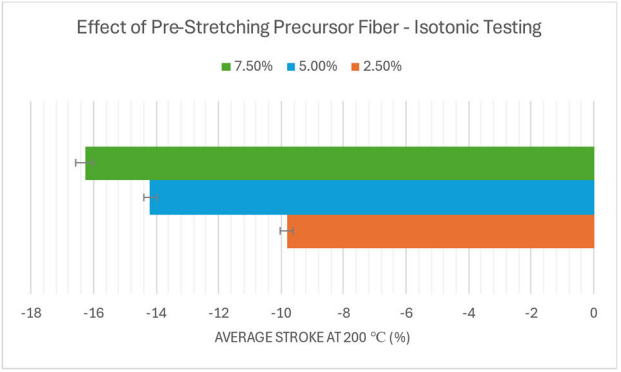

FIGURE 10. Effect of pre-stretching precursor fiber on TCP stroke.

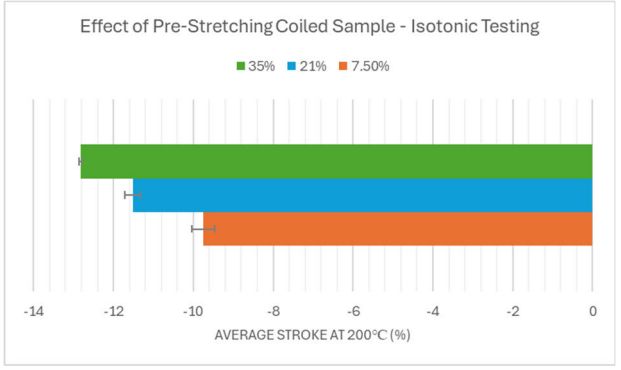

FIGURE 11. Effect of pre-stretching coiled sample on TCP stroke.

APPENDIX B
COMPLETE ISOMETRIC TESTING RESULTS

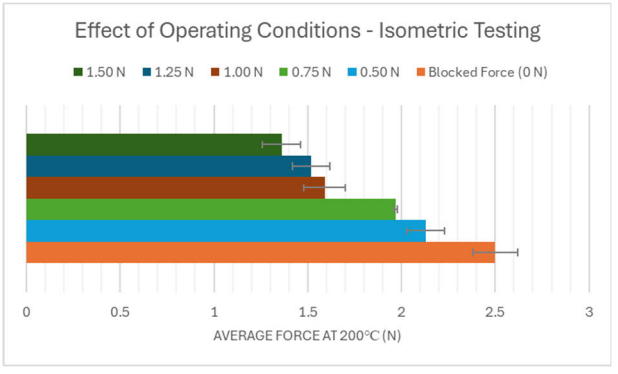

FIGURE 12. Effect of operating pre-stretch on TCP force.

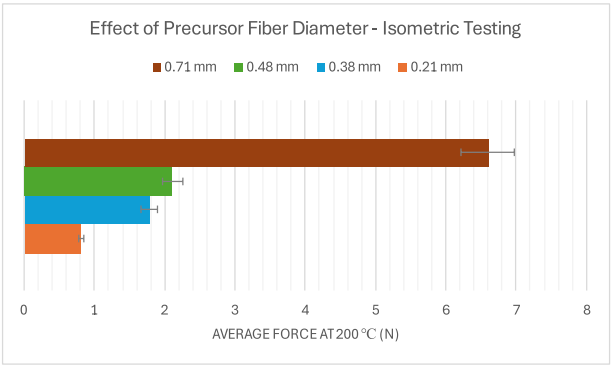

FIGURE 13. Effect of precursor fiber diameter on TCP force.

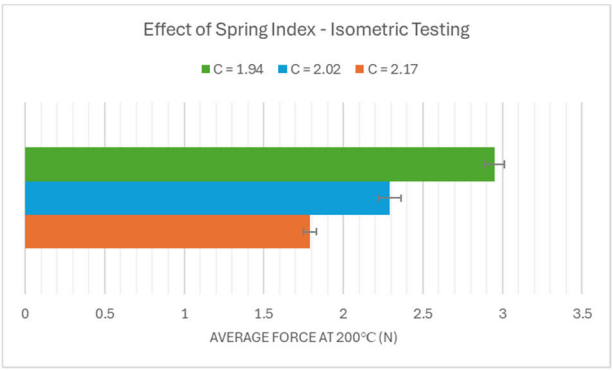

FIGURE 14. Effect of spring index on TCP force.

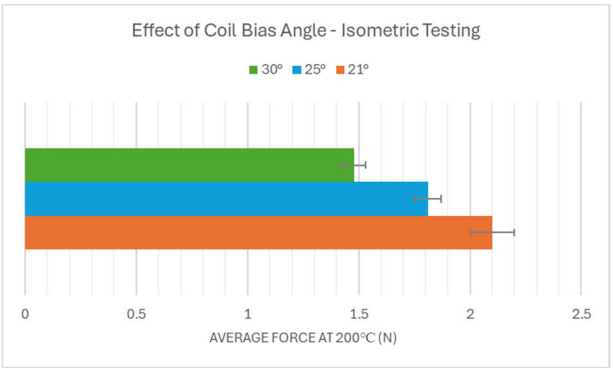

FIGURE 15. Effect of twist density and coil bias angle on TCP force.

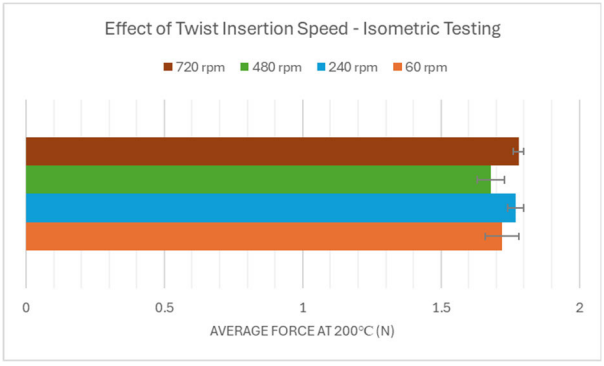

FIGURE 16. Effect of twist insertion speed on TCP force.

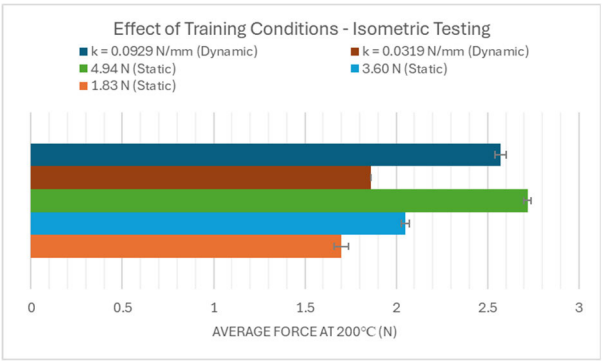

FIGURE 17. Effect of training conditions on TCP force.

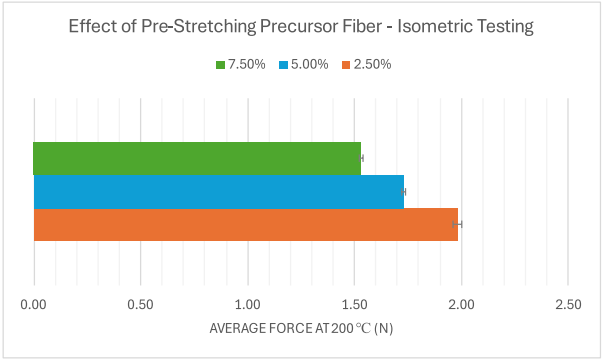

FIGURE 18. Effect of pre-stretching precursor fiber on TCP force.

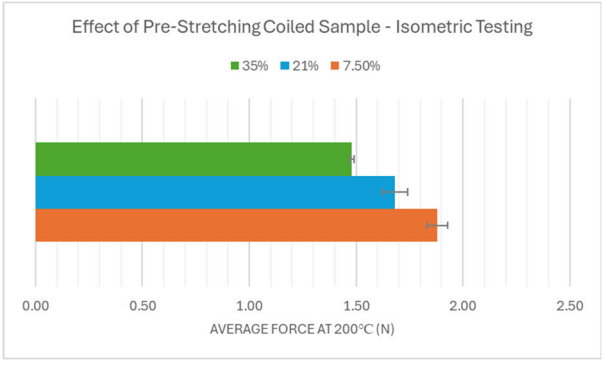

FIGURE 19. Effect of pre-stretching coiled sample on TCP force.

APPENDIX C
COMPLETE ECCENTRIC TESTING RESULTS

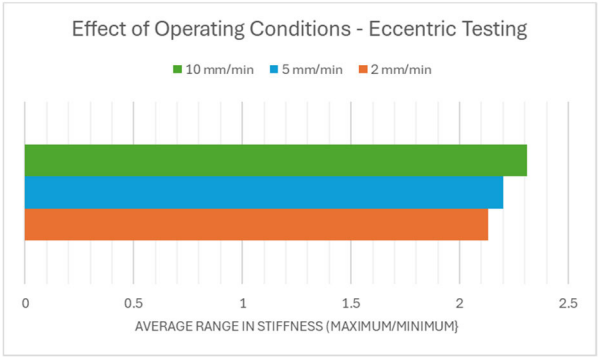

FIGURE 20. Effect of operating strain rate on TCP range in stiffness.

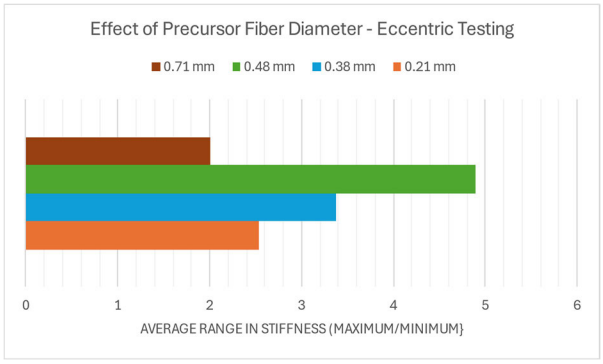

FIGURE 21. Effect of precursor fiber diameter on TCP range in stiffness.

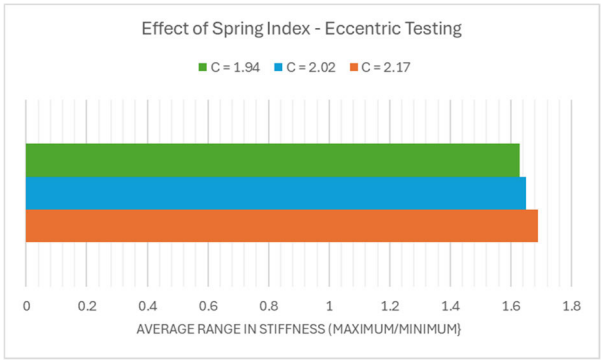

FIGURE 22. Effect of spring index on TCP range in stiffness.

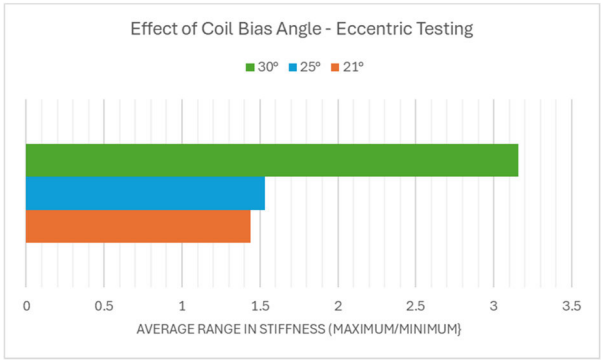

FIGURE 23. Effect of twist density and coil bias angle on TCP range in stiffness.

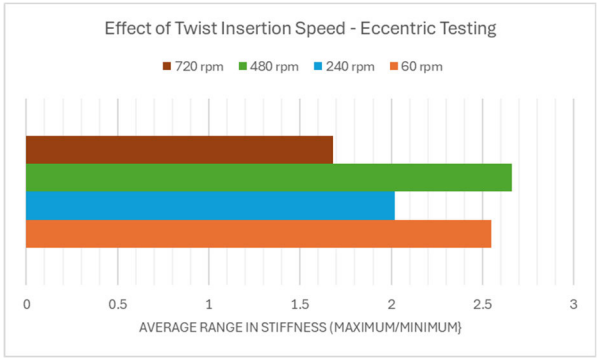

FIGURE 24. Effect of twist insertion speed on TCP range in stiffness.

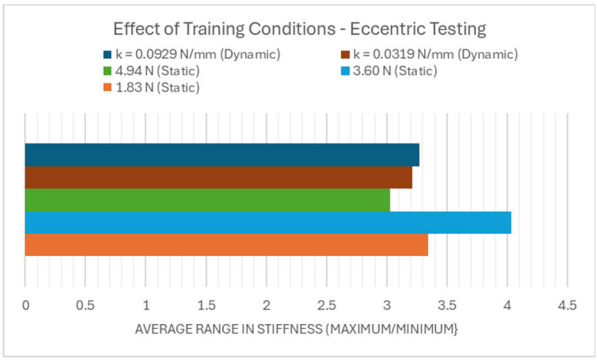

FIGURE 25. Effect of training conditions on TCP range in stiffness.

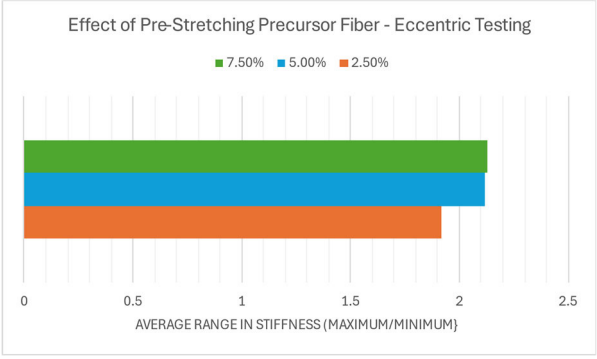

FIGURE 26. Effect of pre-stretching precursor fiber on TCP range in stiffness.

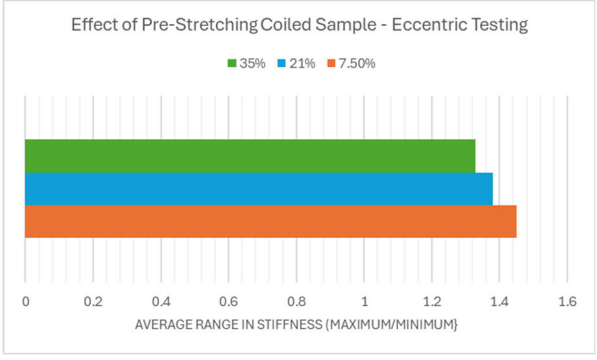

FIGURE 27. Effect of pre-stretching coiled sample on TCP range in stiffness.

ACKNOWLEDGMENT

This research did not receive any specific grant from funding agencies in the public, commercial, or not-for-profit sectors.

Declaration of Competing Interest: The authors report no declarations of interest.

Declaration of Generative AI and AI-Assisted Technologies in the Writing Process: During the preparation of this work the authors did not use any generative AI or AI-assisted technologies. They have reviewed and edited the manuscript and take full responsibility for the content of the publication.

Data Availability: Data supporting the findings in this study can be found in the online version at https://doi.org/10.57760/sciencedb.15686.

REFERENCES

[1] S. M. Mirvakili and I. W. Hunter, "Artificial muscles: Mechanisms, applications, and challenges," *Adv. Mater.*, vol. 30, no. 6, Feb. 2018, Art. no. 1704407, doi: 10.1002/adma.201704407.

[2] B. Jamil, N. Oh, J.-G. Lee, H. Lee, and H. Rodrigue, "A review and comparison of linear pneumatic artificial muscles," *Int. J. Precis. Eng. Manuf.-Green Technol.*, vol. 11, no. 1, pp. 277–289, 2024, doi: 10.1007/s40684-023-00531-6.

[3] C. S. Haines, M. D. Lima, N. Li, G. M. Spinks, J. Foroughi, J. D. W. Madden, S. H. Kim, S. Fang, M. J. de Andrade, F. Göktepe, and Ö. Göktepe, "Artificial muscles from fishing line and sewing thread," *Science*, vol. 343, no. 6173, pp. 868–872, Feb. 2014, doi: 10.1126/science.1246906.

[4] F. Karami and Y. Tadesse, "Modeling of twisted and coiled polymer (TCP) muscle based on phenomenological approach," *Smart Mater. Struct.*, vol. 26, no. 12, Dec. 2017, Art. no. 125010, doi: 10.1088/1361-665x/aa8d7d.

[5] F. Karami, L. Wu, and Y. Tadesse, "Modeling of one-ply and two-ply twisted and coiled polymer (TCP) artificial muscles," *IEEE/ASME Trans. Mechatronics*, vol. 26, no. 1, pp. 300–310, Feb. 2021, doi: 10.1109/TMECH.2020.3014931.

[6] T. Luong, K. Kim, S. Seo, J. H. Park, Y. Kim, S. Y. Yang, K. H. Cho, J. C. Koo, H. R. Choi, and H. Moon, "Impedance control of a high performance twisted-coiled polymer actuator," in *Proc. IEEE/RSJ Int. Conf. Intell. Robots Syst. (IROS)*, Oct. 2018, pp. 8701–8706, doi: 10.1109/IROS.2018.8593937.

[7] S. Liu, X. Tang, D. Zhou, and Y. Liu, "Fascicular module of nylon twisted actuators with large force and variable stiffness," *Sens. Actuators A, Phys.*, vol. 315, Nov. 2020, Art. no. 112292, doi: 10.1016/j.sna.2020.112292.

[8] S. Y. Yang, K. H. Cho, Y. Kim, K. Kim, J. H. Park, H. S. Jung, J. U. Ko, H. Moon, J. C. Koo, H. Rodrigue, J. W. Suk, J.-D. Nam, and H. R. Choi, "Soft fabric actuator for robotic applications," in *Proc. IEEE/RSJ Int. Conf. Intell. Robots Syst. (IROS)*, Oct. 2018, pp. 5451–5456, doi: 10.1109/IROS.2018.8594275.

[9] D. Kongahage, G. M. Spinks, and J. Foroughi, "Twisted and coiled multiply yarns artificial muscles," *Sens. Actuators A, Phys.*, vol. 318, Feb. 2021, Art. no. 112490, doi: 10.1016/j.sna.2020.112490.

[10] B. P. R. Edmonds, "Feasibility of twisted coiled polymer actuators for use in upper limb wearable rehabilitation devices," doctoral dissertation, School Biomed. Eng., Univ. Western Ontario Canada, 2020. [Online]. Available: https://ir.lib.uwo.ca/etd/7544

[11] J. He, J. Li, Z. Sun, F. Gao, Y. Wu, and Z. Wang, "Kinematic design of a serial–parallel hybrid finger mechanism actuated by twisted-and-coiled polymer," *Mechanism Mach. Theory*, vol. 152, Oct. 2020, Art. no. 103951, doi: 10.1016/j.mechmachtheory.2020.103951.

[12] S. Aziz, S. Naficy, J. Foroughi, H. R. Brown, and G. M. Spinks, "Controlled and scalable torsional actuation of twisted nylon 6 fiber," *J. Polym. Sci. B, Polym. Phys.*, vol. 54, no. 13, pp. 1278–1286, Jul. 2016, doi: 10.1002/polb.24035.

[13] S. Aziz, S. Naficy, J. Foroughi, H. R. Brown, and G. M. Spinks, "Effect of anisotropic thermal expansion on the torsional actuation of twist oriented polymer fibres," *Polymer*, vol. 129, pp. 127–134, Oct. 2017, doi: 10.1016/j.polymer.2017.09.052.

[14] C. L. Choy, F. C. Chen, and K. Young, "Negative thermal expansion in oriented crystalline polymers," *J. Polym. Sci., Polym. Phys. Ed.*, vol. 19, no. 2, pp. 335–352, Feb. 1981, doi: 10.1002/pol.1981.180190213.

[15] M. Hiraoka, K. Nakamura, H. Arase, K. Asai, Y. Kaneko, S. W. John, K. Tagashira, and A. Omote, "Power-efficient low-temperature woven coiled fibre actuator for wearable applications," *Sci. Rep.*, vol. 6, no. 1, p. 36358, Nov. 2016, doi: 10.1038/srep36358.

[16] L. Saharan and Y. Tadesse, "Fabrication parameters and performance relationship of twisted and coiled polymer muscles," in *Proc. ASME Int. Mech. Eng. Congr. Expo. (IMECE)*, Phoenix, AZ, USA, Nov. 2016, pp. 1–8, doi: 10.1115/imece2016-67314.

[17] L. Saharan and Y. Tadesse, "Chapter 3—Novel twisted and coiled polymer artificial muscles for biomedical and robotics applications," in *Materials for Biomedical Engineering*, A.-M. Holban and A. M. Grumezescu, Eds., Amsterdam, The Netherlands: Elsevier, 2019, pp. 45–75, doi: 10.1016/B978-0-12-816909-4.00003-8.

[18] Y. Nishimura and G. M. Spinks, "Detailing the visco-elastic origin of thermo-mechanical training of twisted and coiled polymer fiber artificial muscles," *J. Polym. Sci.*, vol. 60, no. 8, pp. 1360–1370, Apr. 2022, doi: 10.1002/pol.20220024.

[19] T. Li, Y. Wang, K. Liu, H. Liu, J. Zhang, X. Sheng, and D. Guo, "Thermal actuation performance modification of coiled artificial muscle by controlling annealing stress," *J. Polym. Sci. B, Polym. Phys.*, vol. 56, no. 5, pp. 383–390, Mar. 2018.

[20] A. Cherubini, G. Moretti, R. Vertechy, and M. Fontana, "Experimental characterization of thermally-activated artificial muscles based on coiled nylon fishing lines," *AIP Adv.*, vol. 5, no. 6, Jun. 2015, Art. no. 067158, doi: 10.1063/1.4923315.

[21] L. Li, W. Ma, Q. Zhang, G. Yuan, H. Li, and Y. Tian, "Research on the mechanism of variable stiffness of the twisted and coiled polymer actuator during saturated contraction," *Smart Mater. Struct.*, vol. 29, no. 6, May 2020, Art. no. 065014, doi: 10.1088/1361-665x/ab85a0.

[22] *Trilene® Big Game™*. Berkley® Fishing. Accessed: Apr. 27, 2024. [Online]. Available: https://www.berkley-fishing.com/trilene-big-game-monofilament-1285546

[23] *Certification of Test*, Instron Corp., Norwood, MA, USA, 1987.

[24] *The Series 96 User's Manual*. Accessed: Apr. 27, 2024. [Online]. Available: https://www.watlow.com/resources-and-support/technical-library/user-manuals?keyw=Series

[25] *Series 240 General Purpose DC–DC LVDTs*. Trans-Tek. Accessed: May 7, 2024. [Online]. Available: https://transtekinc.com/products/series-240/

[26] J. Martin, "Experimental characterization of twisted and coiled polymer actuators," Science Data Bank, Fac. Eng., Dept. Mech. Eng., Univ. Ottawa, Ottawa, ON, Canada, Tech. Rep., Feb. 2024, doi: 10.57760/sciencedb.15686.

JACOB MARTIN received the B.A.Sc. degree in biomedical and mechanical engineering and the M.A.Sc. degree in biomedical engineering from the University of Ottawa, Canada, in 2019 and 2023, respectively. His research interests include soft actuators, artificial muscles, smart materials, and mobility assistive devices.

MARC DOUMIT received the B.S. degree in mechanical engineering, the M.Eng. degree in engineering management, and the Ph.D. degree in mechanical engineering from the University of Ottawa, Canada, in 2000, 2003, and 2009, respectively. He currently holds the position of an Associate Professor and an Associate Chair with the Mechanical Engineering Department, University of Ottawa. His research focuses on smart and soft actuators, exoskeletons, prosthetic and orthotic limbs, and bio-inspired designs.